


Particle-Based Assembly Using Precise Global Control

Jakob Keller 

Department of Computer Science, TU Braunschweig, Germany
jkeller@ibr.cs.tu-bs.de

Christian Rieck 

Department of Computer Science, TU Braunschweig, Germany
rieck@ibr.cs.tu-bs.de

Christian Scheffer 

Department of Computer Science, WWU Münster, Germany
christian.scheffer@uni-muenster.de

Arne Schmidt 

Department of Computer Science, TU Braunschweig, Germany
aschmidt@ibr.cs.tu-bs.de

Abstract

In micro- and nano-scale systems, particles can be moved by using an external force like gravity or a magnetic field. In the presence of adhesive particles that can attach to each other, the challenge is to decide whether a shape is constructible. Previous work provides a class of shapes for which constructibility can be decided efficiently, when particles move maximally into the same direction on actuation.

In this paper, we consider a stronger model. On actuation, each particle moves one unit step into the given direction. We prove that deciding constructibility is NP-hard for three-dimensional shapes, and that a maximum constructible shape can be approximated. The same approximation algorithm applies for 2D. We further present linear-time algorithms to decide whether a tree-shape in 2D or 3D is constructible. If scaling is allowed, we show that the c -scaled copy of every non-degenerate polyomino is constructible, for every $c \geq 2$.

2012 ACM Subject Classification Theory of computation \rightarrow Randomness, geometry and discrete structures

Keywords and phrases Programmable Matter · Tile Assembly · Tilt · Approximation · NP-Hardness

Related Version This is the full version of an extended abstract that will appear in the 17th Algorithms and Data Structures Symposium (WADS 2021) August 9-11, 2021.

Supplement Material 3D models: <https://gitlab.ibr.cs.tu-bs.de/alg/particle-based-assembly-extra>

Acknowledgements We thank Linda Kleist for valuable discussions and suggestions that improved the presentation of this paper, Matthias Konitzny for the awesome 3D images, and the anonymous reviewers for providing helpful comments.

1 Introduction

In recent years, the easier access to micro- and nano-scale systems has given rise to challenges that deal with programmable matter. In some of these applications, particles can be controlled by a global external force such as gravity or a magnetic field. On actuation, every particle moves into the same direction at unit speed. Assembly of particles into desired structures using maximal movements, i.e., every particle moves into a given direction until it hits an obstacle or another particle, has been investigated in [2, 3, 8, 39]. However, it is also reasonable to expose the particles to these forces just for a limited amount of time, such that

more precise movements become possible. Reconfiguration of a set of particles [2], gathering all particles [7, 31], or assembling patterned rectangles [13] are well studied problems.

In this paper, we consider the construction of tile-based structures (such as polyominoes in 2D, polycubes in 3D) through adhesive particles, that all move one step into the same direction on actuation. Whenever two particles come close, they stick together. In this model, we consider the problem of deciding whether a given shape is constructible. For definitions see Section 2.

SINGLE STEP TILT ASSEMBLY PROBLEM (STAP)

Given a shape P (polyomino in 2D or polycube in 3D), does there exist a sequence of tile moves to construct P ?

We denote the problem in 2D and 3D by 2D-STAP and 3D-STAP, respectively. The optimization variant of STAP, called MAXSTAP, asks for a constructible subshape $P_{\max} \subset P$ of maximum size.

1.1 Our Contributions

We show the following results.

- 3D-STAP is NP-hard, see Theorem 7.
- In dimension $d = 2, 3$, there is an $\Omega(|P|^{-1/d})$ -approximation algorithm for MAXSTAP, see Theorem 11 and Corollary 12.
- For tree-shapes in 2D and 3D, there is a linear-time algorithm for STAP, see Theorem 15 and Corollary 16.
- For every non-degenerate polyomino P , the 2-scaled copy of P is constructible, see Theorem 22, and for every non-degenerate polycube P , the 7-scaled copy of P is constructible, see Theorem 24.

1.2 Related Work

We divide the related work into three categories: Algorithmic results in tile self-assembly and tilt problems, and practical approaches.

Self-Assembly

Instead of relying on universal, external control of agents, it is possible to use DNA as material. DNA-strands can either be used to fold into the desired shape [37], or to create building blocks based on *Wang tiles* [45] that can then again self-assemble into shapes in a non-deterministic way [38, 47]. Instead of considering the case where all DNA tiles are binding to a seed assembly, it is also natural to consider multiple seeds that simultaneously grow subassemblies which can then again attach to each other. This 2-handed tile self-assembly model [16] can also be used to let the subassemblies connect in phases, i.e., in a hierarchical manner; this is sometimes also called staged tile self-assembly [17, 18, 21, 23, 24, 40]. For more details on algorithmic self-assembly, we refer to the surveys by Doty [25], Patitz [34], and Woods [48].

Tilt Problems

The process of self-assembly works by diffusion and is non-deterministic. If a deterministic approach is desired, we can use global control to move particles into different directions. Using global control opens a wide field of problems, that we summarize briefly.

If an obstacle environment can be designed, Becker et al. [6] show that particles can be used for computation by implementing NOT, NAND, NOR, XOR and XNOR gates. If the model is generalized by adding 2×1 particles (dominoes), it is also possible to construct FAN-OUT gates [5, 41].

Mahadev et al. [31] show how to gather n particles within an obstacle environment in $O(n^3)$ actuation steps. Becker et al. [7] improve the runtime to only depend on the geometric complexity of the workspace, rather than on the number of particles.

Closely related to this problem are occupancy, relocation and reconfiguration problems. For a given set of particles within an obstacle environment, these problems ask for a sequence of tilts such that (i) any particle reaches a designated position, (ii) a specific particle reaches a designated position, and (iii) every particle reaches its respective target position. If particles are allowed to move a unit step on actuation, Caballero et al. [14] show that (i) permits a linear-time algorithm, while the decision variants of (ii) and (iii) are NP-hard. More recently, Caballero et al. [15] show PSPACE-completeness for (ii). Becker et al. [4] show that (i) is NP-hard when particles have to move maximally. Balanza-Martinez et al. [2] give tighter results by proving PSPACE-completeness for all three problems, when maximal movement is considered.

All these papers have in common that particles do not stick to each other. Manzoor et al. [32] provide algorithms for assembling shapes, called *drop shapes*, from *sticky* particles under global control. In this assembly process, only one particle at a time is added by maximal movements to a seed assembly. They also show that the assembly process can be pipelined, i.e., the same shape is produced multiple times. Becker et al. [8] prove that every drop shape permits an amortized construction time of $O(1)$, provided that sufficiently many copies are constructed. However, every shape needs a custom-designed obstacle workspace. Balanza-Martinez et al. [3] designed a single obstacle workspace in which every drop shape can be constructed, if it fits in a $w \times h$ rectangle. By using not only single particles but whole subassemblies, the class of constructible shapes increases (see [2, 39]). A crucial step is to decompose a given shape into two connected parts, that can then be pulled apart into a single direction, without causing collisions. Agarwal et al. [1] recently proved that this problem is NP-hard, even if a direction is given.

Another problem that arises from a practical point of view is error detection. Keldenich et al. [28] show that ortho-convex shapes can be classified within an obstacle workspace, i.e., these shapes can be tested for errors during the assembly process.

Practical Approaches

On the practical side, there are multiple approaches related to the assembly of micro-structures with uniform movement. Related work on controlling a swarm of particles, especially in biological or medical environments, include control by electricity [12], chemical reactions [46], light [42, 46] and magnetism. Because magnetic resonance imaging (MRI) scanners already employ magnetism in a clinical context, it is reasonable to design a magnetic control device based on MRI scanners [9, 19, 33, 43, 44]. Another advantage of using MRI scanners lies in the possibility of tracking the positions of the agents as well as moving them. If the devices provide stronger custom coils, this approach might even lead to new applications where tissue penetration is wanted [10]. There are different types of particles discussed in the literature. On the one hand, there is research in which single cell organisms (*Tetrahymena Pyriformis*) are fed with iron particles so that they can be steered by applying a magnetic field [11, 29, 30]. On the other hand, research considers the fabrication of artificial micro-swimmers. These are usually called *Artificial Bacterial Flagella* (ABF) because they resemble

their natural counterpart [26]. Another very popular approach is to design ABFs that consist of a magnetic head, that can be turned by a revolving magnetic field, and a rigid helical tail [20, 27, 35, 36, 49, 50]. By quickly turning the micro-swimmer, the tail generates a thrust force by its corkscrew shape.

2 Preliminaries

Polyomino. Let $P \subset \mathbb{Z}^2$ be a finite set of N grid points in the plane. The grid points of \mathbb{Z}^2 are called *positions*. The embedded graph G_P is the grid graph induced by P , in which two vertices are adjacent if they are at unit distance. If G_P is connected, we obtain a *polyomino* by placing a unit square, called *tile*, centered on every vertex of G_P . Two tiles are *adjacent*, if their respective vertices in G_P are adjacent, i.e., they share an edge. A position $p \in \mathbb{Z}^2$ is *occupied*, if there is a tile that is placed on p , and *free* otherwise. The neighborhood $N[\cdot]$ of a tile or position is the respective set of adjacent positions. A polyomino P is *simple*, if the grid graph $\mathbb{Z}^2 \setminus G_P$ is connected. If there are at least two tiles $t_1, t_2 \in P$ that share a common point but for which there is no tile in $N[t_1] \cap N[t_2]$, P is called *degenerate*. If G_P is a tree, the respective polyomino is *tree-shaped*.

Workspace. The *workspace* is a rectangular region of $2N \times 2N$ positions, anchored at position $(0, 0)$. The workspace contains a *seed tile* at position (N, N) .

Construction Step. A tile can *move* from one position p to an adjacent position q as long as the neighborhood $N[p]$ is free. A *construction step* is a sequence σ of moves such that σ moves a tile to a position adjacent to an occupied position. Without loss of generality, we assume that every construction step starts at position $(0, 0)$. Analogously, we define a *deconstruction step* as a sequence $\tilde{\sigma}$ that moves a tile from its position to the position $(0, 0)$. If there is a deconstruction step for a tile t , we call t *removable*.

Constructibility. Beginning with a seed tile, a polyomino P with N tiles, is constructible if and only if there is a *construction sequence* $\Sigma = (\sigma_1, \sigma_2, \dots, \sigma_N)$ of N consecutive construction steps such that the resulting polyomino P' , induced by successively adding tiles with Σ , is equal to P . Reversing Σ yields a *deconstruction sequence* $\tilde{\Sigma}$, i.e., a sequence of tiles getting removed from P .

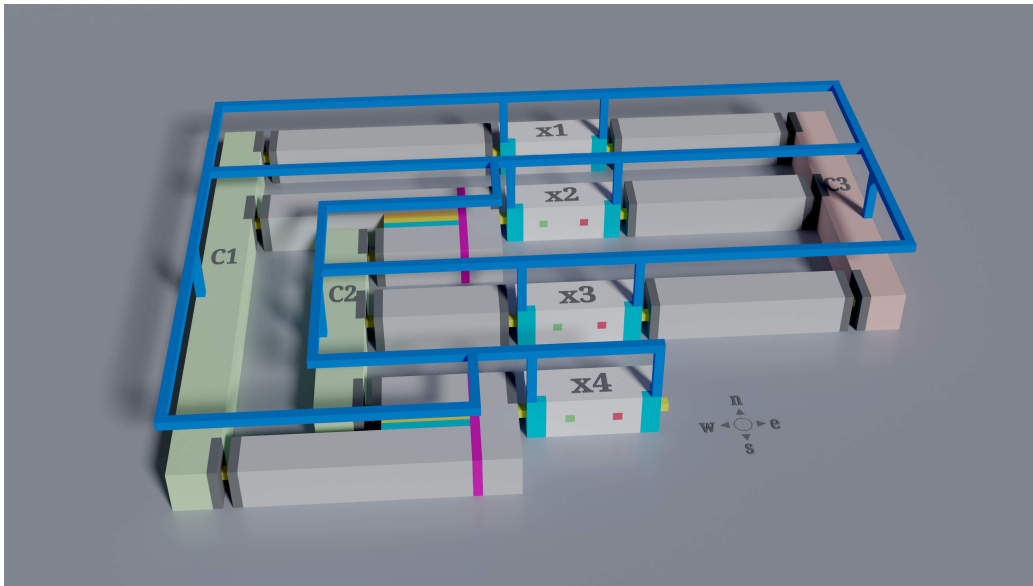
Note that the definitions are given for a 2D setting. It is straightforward to extend these to the 3D setting, by letting $P \subset \mathbb{Z}^3$, introducing two additional directions in that a tile can move, and considering unit cubes instead of unit squares as tiles, and anchoring the workspace, that contains a seed tile at position (N, N, N) , at position $(0, 0, 0)$.

Firstly, we restate a result by Becker et al. [8] for the full tilt assembly model in two dimensions, which can easily be adapted for the single step model considered in this paper, as well as it applies (in both models) in the 3D setting.

► **Theorem 1** (Theorem 2, [8]). *A polyomino P can be constructed if and only if it can be deconstructed using a sequence of tile removal steps that preserve connectivity. A construction sequence is a reversed deconstruction sequence.*

3 NP-Hardness of 3D-STAP

Becker et al. [8] showed that it is NP-hard to decide whether or not a polycube is constructible in the full tilt model. However, our model is more powerful and we cannot adapt their proof. In this section, we show that 3D-STAP is NP-hard. The proof is based on a reduction from the NP-hard problem PLANAR MONOTONE 3SAT [22]. This problem asks to decide whether



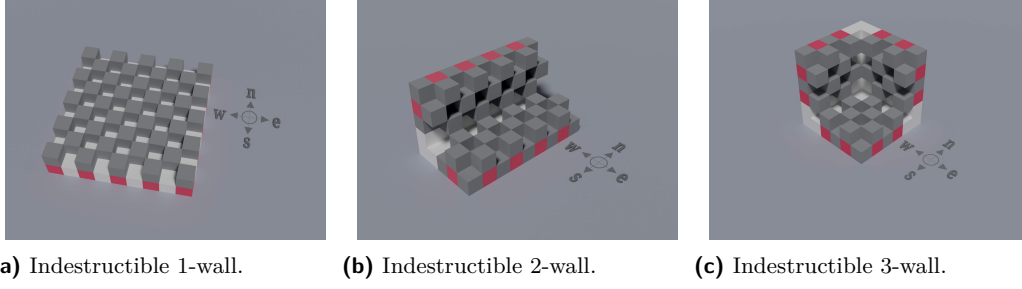
■ **Figure 1** Symbolic overview of the NP-hardness reduction. The instance is due to the PLANAR MONOTONE 3SAT formula $\varphi = (x_1 \vee x_2 \vee x_4) \wedge (x_2 \vee x_3 \vee x_4) \wedge (\overline{x_1} \vee \overline{x_2} \vee \overline{x_4})$. The variable gadgets are shown in white, while the positive and negative clause gadgets are shown in green and red, respectively. The gray cuboids represent connector gadgets. The ‘colorful lines’ are representing conjunction gadgets. All clauses and variables are connected by a blue frame above the construction.

a Boolean 3-CNF formula φ is satisfiable, for which in each clause the literals are either all positive or all negative, and for which the clause-variable incidence-graph is planar. Because of Theorem 1, we will argue that a polycube is deconstructible if and only if a Boolean 3-CNF formula is satisfiable.

3.1 Outline of the NP-Hardness Reduction.

For every instance φ of PLANAR MONOTONE 3SAT, we construct a polycube P_φ as an instance of 3D-STAP. We consider a rectilinear planar embedding of the variable-clause incidence graph G_φ of φ where the variable vertices are placed on a line, and clauses containing positive and negative literals are placed on either side, respectively. For a schematic overview of P_φ , consider Figure 1. In P_φ , each variable and each clause of φ is represented by a variable gadget and a clause gadget, respectively. To realize the fact that a variable can be contained in several clauses, we introduce a conjunction gadget. An edge in G_φ is realized by a connector gadget. To guarantee connectivity during the deconstruction of the polycube P_φ , we need to make sure that parts of the variable gadgets that are not participating in the satisfying assignment, are not disconnected in several parts. Therefore, we add a frame above the actual polycube, connecting all clauses with certain parts of the variable gadgets.

We can show that there is a deconstruction sequence for P_φ if and only if φ is satisfiable. By using a checkered tile arrangement within all gadgets, we can enforce a specific deconstruction sequence. On the one hand, we ensure that, due to the connectivity constraint, either the part of the variable that is connected to their positive or to their negative literal containing clauses can be deconstructed; thus, these deconstruction steps can be used to determine a valid variable assignment for φ . This implies that, together with the conjunction gadgets, all clauses containing the respective literal can be deconstructed. On the other hand, the



■ **Figure 2** Indestructible walls. Red cubes indicate the respective positions of teeth.

other side of the variable gadget can only be deconstructed, if all other clauses are already deconstructed, i.e., if the clauses are satisfied by other variable assignments.

3.2 Construction of the Gadgets.

In the following, we describe polycubes serving as gadgets in the NP-hardness reduction. In particular, we need polycubes for variables and clauses, as well as for (logic) conjunction. Furthermore, we need a gadget to connect several gadgets with each other, i.e., a connector gadget. All gadgets are based on the following polycube that cannot be deconstructed if we restrict the deconstruction direction.

Indestructible Wall. A *wall* is the polycube depicted in Figure 2(a). It consists of two layers, an odd dimensional *solid layer*, and a checkered *tooth layer*. This tooth layer consists of non-adjacent cubes (shown as gray cubes) at even positions. This construction can simply be modified to construct a *k-wall*, see Figure 2 for examples. Note that k can be at most 6, and there exist several k -walls for $k \in \{3, 4\}$.

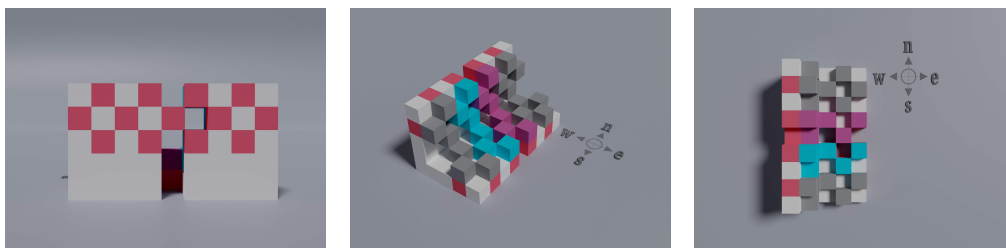
Recall that a deconstruction step is a sequence of moves that moves a tile of the polycube to position $(0, 0, 0)$. We want to show that a wall is *not deconstructible from a specific direction*, in particular from the solid layer. To do so, we assume that the workspace is designed such that $(0, 0, 0)$ is below the wall and that there is no path that starts from above the wall, bypasses it and eventually reaches $(0, 0, 0)$.

► **Lemma 2.** *A k -wall, $k \in \{1, \dots, 6\}$, is not deconstructible from its solid layers.*

Proof. Suppose for the sake of a contradiction that a k -wall is deconstructible from its solid layers, and let $\tilde{\Sigma} = (\sigma_1, \dots, \sigma_N)$ be a deconstruction sequence. Because we only have access to the solid layers, σ_1 has to remove a cube from a solid layer. We partition the solid layer in cubes at even and odd positions. Because there are cubes in the tooth layer at even positions, we can only remove cubes at odd positions from the solid layer to maintain connectivity. But then there cannot be a $\tilde{\sigma}_i \in \tilde{\Sigma}$ such that $\tilde{\sigma}_i$ removes a cube from the tooth layer. This is a contradiction to the existence of $\tilde{\Sigma}$. Thus, a wall is not deconstructible from the solid layer. ◀

We show that the specific design of the tooth layers of a k -wall is necessary to guarantee the indestructibility, i.e., if at least one tooth is missing, the resulting polycube is deconstructible from the solid layer.

► **Lemma 3.** *There is at least one position p at a tooth layer of a k -wall, $k \in \{1, \dots, 6\}$ such that the k -wall is deconstructible from the solid layer if p is free.*



■ **Figure 3** Different views on a disconnected 2-wall.

Proof. Let p be the position of the missing tooth, and consider the respective position in the solid layer. Removing this tile and the four adjacent tiles will yield in a hole that is large enough that tiles can pass through it. Thus, tiles from the tooth layer can be removed. To do so, we position a tile from the tooth layer above p and move it in the direction of the hole such that there will be no face contact to other tiles. Thus, all teeth can be removed one by one, followed by deconstructing the remaining parts of the solid layer. ◀

A simple observation is that these k -walls can arbitrarily be enlarged without losing the property of being indestructible. Of particular interest for the reduction are enlarged 6-walls, called *cuboids*, that will serve as *clause* and *connector gadgets*.

Another crucial observation is that because a k -wall is not deconstructible from its solid layers, we can leave out several cubes of the solid layers so that the remaining shape is disconnected into two parts, see Figure 3. This insight will lead to a configuration that allows for a decision, i.e., that will serve as the variable gadget.

If two cuboids have to be connected, we place them at distance one to each other and add a single cube to connect them. Furthermore, we remove cubes at matching sides in a 3×3 area such that we can move cubes from the inside of one cuboid to the other through these holes, see Figures 4(c) and 4(d) for illustration.

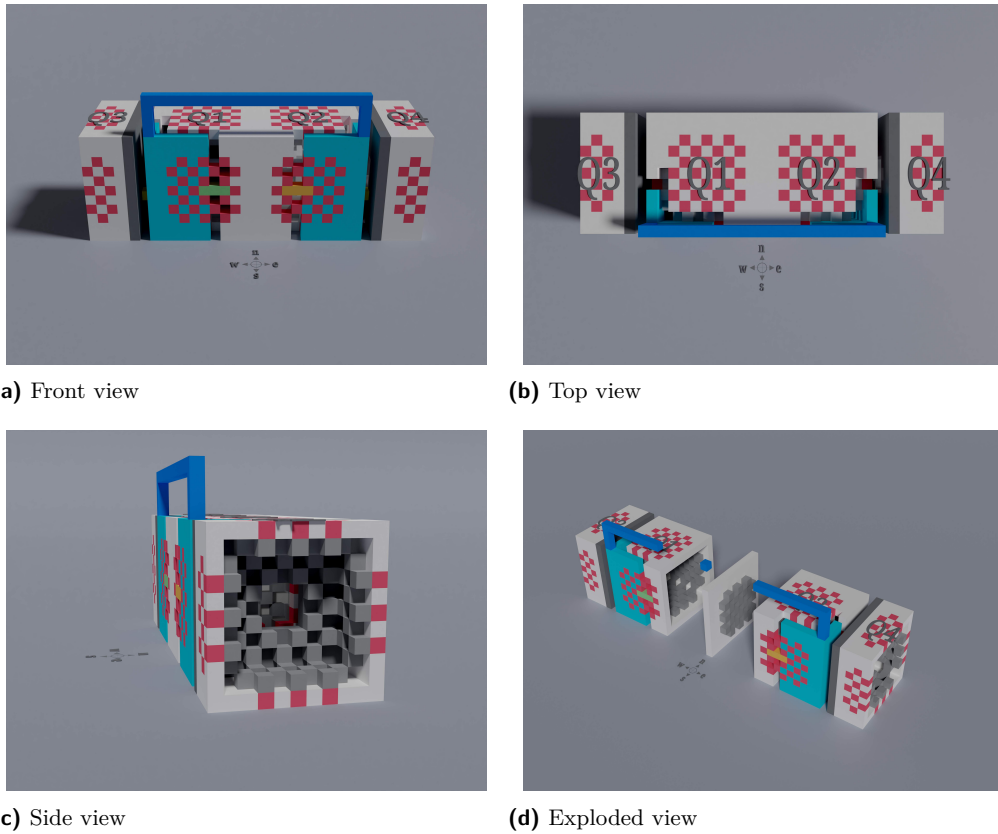
Variable Gadget. The variable gadget consists of two indestructible cuboids (Q_1 and Q_2) that share a solid layer, see Figure 4(d) for an exploded illustration. As shown in Figure 4, we remove tiles (similar to Figure 3) to separate an L-shaped part of each cuboid (light blue tiles). These shapes are then reconnected by two bridges (green and orange tiles), see Figure 4(a). Additionally, the L-shaped parts are connected by a thin frame above the cuboids (dark blue tiles).

▷ **Observation 4.** Solely removing the green and orange tiles of a variable gadget results in a disconnected shape.

As a consequence of Observation 4, the forced choice of removing either the green or the orange tiles, can be used to determine an assignment for the respective Boolean variable. It remains to show how a variable gadget can be deconstructed, if additional cuboids are attached at each side.

► **Lemma 5.** *Let P be a polycube that is put together by a variable gadget and one cuboid (Q_3 and Q_4) at each end, connected to the respective L-shaped parts. Then P is only deconstructible if at least Q_3 or Q_4 is deconstructible.*

Proof. Without loss of generality, let Q_3 be deconstructible. Then the orange tiles can be removed in order to deconstruct Q_4 (by Lemma 3), and Q_2 afterwards. Due to the hole between Q_1 and Q_3 and the assumption that Q_3 is deconstructible, Q_1 can also be deconstructed.



■ **Figure 4** Different views on the variable gadget.

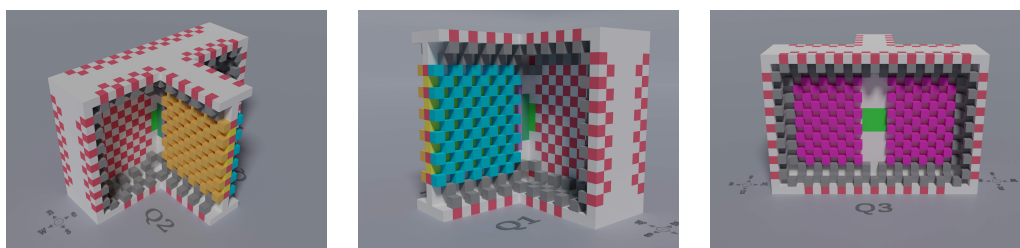
On the other hand, if neither Q_3 nor Q_4 is deconstructible, only the green or the orange tiles can be removed (by Observation 4). But then, either Q_3 or Q_4 can be deconstructed, but not both, resulting in an indestructible shape. ◀

As the last ingredient for our NP-hardness reduction we need a gadget that realizes a conjunction. This gadget will be used to guarantee that a variable gadget can be completely deconstructed if and only if all clauses in which the respective variable participates, are satisfied.

Conjunction Gadget. As illustrated in Figure 5, the conjunction gadget is T-shaped. The wall between the cuboids Q_1 and Q_2 contains teeth to both sides, whereas the wall at cuboid Q_3 has teeth except for the positions where the T-shape is connected. This connection will be the crucial part to deconstruct this gadget. At all three positions (Q_1 , Q_2 , and Q_3) we attach connector gadgets leading either to another conjunction, to a variable, or to a clause gadget. Note that these connector gadgets have the same size as the conjunction gadget, i.e., the solid layers of the connectors and the conjunction gadget match.

We can show that this gadget is deconstructible if and only if the cuboid at Q_3 , or both cuboids at Q_1 and Q_2 are deconstructible.

► **Lemma 6.** *Let P be a polycube that is put together by three cuboids Q_1 , Q_2 , and Q_3 which are connected by a conjunction gadget. Then P is deconstructible if and only if Q_1 and Q_2 are both deconstructible, or Q_3 is deconstructible.*



■ **Figure 5** Different views on the conjunction gadget.

Proof. For the proof, we distinguish two cases.

Let Q_1 and Q_2 be deconstructible. Thus, all teeth from the respective insides can be removed. After this, the wall that is shared by Q_1 and Q_2 , becomes deconstructible. Afterwards, by removing the purple, dark green and light green tiles, we create a hole to reach the inside of Q_3 that makes Q_3 deconstructible as well. Thus, P is deconstructible.

Now assume that either Q_1 or Q_2 is deconstructible, but not both. Without loss of generality consider Q_1 to be deconstructible. Then all teeth from its inside can be removed. By this, neither Q_2 nor Q_3 become deconstructible because the teeth on the respective sides do not permit the removal of a enough tiles such that tiles from the respective insides can pass through. Thus, P is not deconstructible.

It remains to show that P is deconstructible if Q_3 is. Because Q_3 is deconstructible, we can remove the teeth at this side of the conjunction gadget. Because there are no teeth at the opposite sides, the whole wall can be deconstructed. This results in holes to the inside of Q_1 and Q_2 such that these cuboids become deconstructible as well. ◀

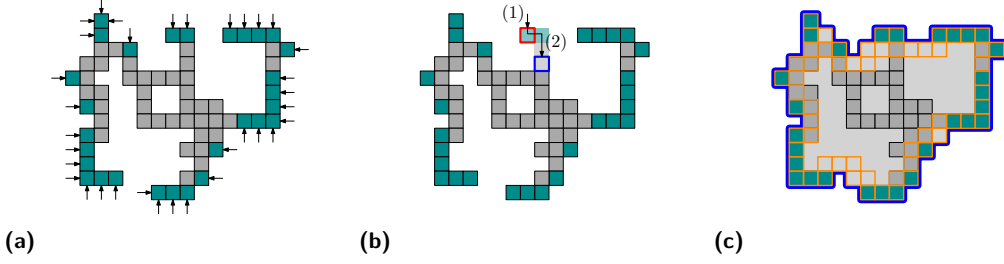
By putting all these together, we obtain the following.

► **Theorem 7.** *3D-STAP is NP-hard.*

Proof. Consider a rectilinear planar embedding of the variable-clause incidence graph G_φ of a given PLANAR MONOTONE 3SAT formula φ , where the variable vertices are placed horizontally in a row, and clauses containing positive and negative literals are placed above and below this row, respectively. We place a variable gadget for every variable (white in Figure 1), and a cuboid for each clause (green in Figure 1). These blocks are connected via connector cuboids (gray) and conjunction gadgets whenever the number of positive or negative occurrences of a variable is larger than one. On top of this construction, we use a frame to hold all clauses and L-shaped parts in the variable gadgets together. This will be necessary to deconstruct the shape completely whenever the underlying 3Sat formula is satisfiable.

▷ **Claim 8.** If there is a deconstruction sequence $\tilde{\Sigma}$ for P_φ , then there is a satisfying assignment for φ .

In order to deconstruct a clause gadget, at least (parts of) one of its literal containing variable gadgets has to be already deconstructed. Thus, every deconstruction sequence has to begin with deconstruction steps that remove either the green or orange tiles from any variable gadget. As argued in Observation 4, not both, the green and orange tiles can be removed, i.e., setting a variable to true and false simultaneously is not possible. Because $\tilde{\Sigma}$ is a deconstruction sequence, eventually each clause will be deconstructed.



■ **Figure 6** (a) Boundary tiles (dark cyan) and non-boundary tiles (gray). (b) Every step of the algorithm adds a tile in two steps: (1) Move a new tile t to a boundary position p of P that is free. (2) Move t on P from p to a position that is adjacent to a tile of the current polyomino P' . (c) The curve B (blue), and the set T (orange).

Therefore, there is a satisfying assignment for φ given by the order in which each variable of P_φ is deconstructed by $\tilde{\Sigma}$. In particular, for each $x_i \in \varphi$, we set $x_i = 1$ if the respective green tiles are removed first, and $x_i = 0$ otherwise.

▷ **Claim 9.** If the Boolean formula φ is satisfiable, then P_φ is deconstructible by some deconstruction sequence $\tilde{\Sigma}$.

Let α be a satisfying assignment of φ . Then the polycube P_φ can be deconstructed as follows: According to whether a variable is set to true or false in α , either the green or orange tiles are removed, respectively. These deconstruction steps produce holes, large enough for a deconstruction of the whole literal representing cube, as argued in Observation 4. Afterwards, because there is a hole from the clause cuboids to the literals, all clauses that contain these literals can be deconstructed by Lemma 3. Because α is a satisfying assignment for φ , all clause gadgets and the respective parts of the variable gadgets can be deconstructed. The respective parts of the variable gadgets that are not participating in the satisfying assignment are connected by the overlaying connectivity frame. Because the clauses are already deconstructed, there are holes through which the remaining parts of the variable gadgets can be deconstructed. Removing the connectivity frame results in deconstructing P_φ .

These two claims complete the proof. ◀

4 Optimization Variant and Approximation

For polyominoes and polycubes that cannot be constructed, it is natural to consider the problem of maximizing a constructible subshape. We show that for each shape P , a portion of $\Omega(|P|^{(d-1)/d})$ can always be constructed, implying a $\Omega(|P|^{-1/d})$ -approximation of MAXSTAP, where d denotes the dimension.

► **Definition 10.** The maximum constructibility of a polyomino P is the ratio $|P_{\max}|/|P|$ where $P_{\max} \subseteq P$ is a constructible polyomino of maximum size.

► **Theorem 11.** In dimension $d = 2, 3$, each d -dimensional polyomino P has a maximum constructibility of at least $\Omega(|P|^{-1/d})$.

Proof. We prove the theorem by showing that greedily filling up accessible empty positions leads to a polyomino $P' \subseteq P$ with $|P'|/|P| \in \Omega(|P|^{-1/d})$. A position p is *accessible* with respect to a polyomino P if we can move a tile t to this position such that t is never adjacent to a tile of P unless t lies on p . A tile $p \in P$ is a *boundary tile* of P if p is accessible with respect

to $P \setminus \{p\}$, see Figure 6(a). If there is a boundary tile p of P that is not part of P' , we add a new tile t to P' in two steps, see Figure 6(b): (1) We move t to the position p . (2) We move t on P to a position adjacent to a tile of P' . This implies that the greedy algorithm ends up with a polyomino holding all boundary tiles of P .

Next, we show a lower bound on the boundary tiles of P of $\Omega(N^{d-1})$. We only consider $d = 2$, a similar surface-volume-argument holds for $d = 3$. Let B be the union of all edges lying between an accessible and a non-accessible position with respect to P , see blue curve in Figure 6(c). B is a non-self-intersecting curve, by the definition of accessible positions. Thus, B partitions the plane into a bounded area A containing P and an unbounded area. Let T be the union of all positions from A sharing at least a corner with B , see the orange positions in Figure 6(c). Then $|T| \geq \sqrt{|A|}$. Note that not each position of T is occupied by P , see the light gray positions in Figure 6(c). Let T' be the positions along B that share an edge with B . It is easy to see that $2|T'| \geq |T|$. Each position p from T' that is not a boundary tile from P is adjacent to a boundary tile p' from P . We call p' a *blocking tile* of p . Each boundary tile is a blocking tile for a constant number of positions $p \in T'$ that are not a boundary tile. Hence, there are $\Omega(|T'|)$ many positions from T' that are not a boundary tile implying that $\Omega(|T'|) = \Omega(|T|)$ tiles from T are boundary tiles. Because $P' \subset A$, we obtain $|P'| \leq |A|$ implying $|T| \in \Omega(\sqrt{|A|}) = \Omega(\sqrt{|P'|})$. Hence, P' has at least $\Omega(N^{1/2})$ boundary tiles. ◀

Theorem 11 implies the following.

► **Corollary 12.** *In dimension $d = 2, 3$, the greedy algorithm is an $\Omega(|P|^{-1/d})$ -approximation for MAXSTAP.*

5 Efficient Algorithms for Special Classes

5.1 Tree Shapes

We can show that STAP can be decided in linear time for tree-shaped polyominoes by a greedy algorithm. Because the removal of a tile with more than one neighbor results in splitting the polyomino in several parts, we are restricted to remove tiles with exactly one neighbor, i.e. leaves. If there are any tiles left, but no further tile can be removed, we conclude that the polyomino cannot be constructed.

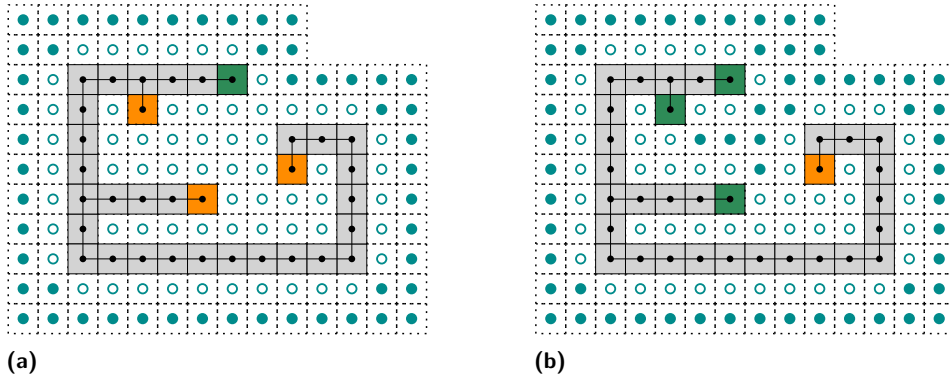
We begin by stating two facts about removable tiles. Firstly, by removing a tile, other tiles do not lose their property to be removable. And secondly, if a tree-shaped polyomino is constructible, then after removing any removable tile, the resulting polyomino is also constructible.

► **Lemma 13.** *Let P be a tree-shaped polyomino and \mathcal{R}_P the set of removable tiles of P . For all $P' \subseteq P$ it holds that if $t \in \mathcal{R}_P \cap P'$, then $t \in \mathcal{R}_{P'}$.*

Proof. Let $t, t' \in \mathcal{R}_P$ and $P' := P \setminus \{t'\}$. Due to the definition of \mathcal{R}_P , P' is connected. Furthermore, the path that removes t from P still exists, because the removal of t' cannot block this path. Therefore, $t \in \mathcal{R}_{P'}$. ◀

► **Lemma 14.** *Let P be a constructible tree-shaped polyomino and t a removable tile. Then, $P \setminus \{t\}$ is also constructible.*

Proof. For the sake of a contradiction, let $P' \subsetneq P$ with $t \in P'$ be the largest constructible polyomino that results through removal of tiles from P and for which $P' \setminus \{t\}$ is constructible.



■ **Figure 7** (a) A polyomino P (gray) and the dual graph of P (black). Tiles in green are removable, tiles in orange are leaves that are not removable yet. Cyan dots represent empty positions with the state ‘available’, cyan circles represent empty positions with the state ‘init’. (b) The situation after the removal of the green tile in (a).

Let t' be the last tile that was removed from P to obtain P' . Because of Lemma 13, we can first remove t from $P' \cup \{t'\}$ and then t' . Thus, P' was not the largest polyomino. ◀

By using Lemma 14 iteratively, we obtain a simple strategy that decides whether a tree-shaped polyomino is constructible or not. By applying suitable subroutines and data structures, this yields a linear-time algorithm.

► **Theorem 15.** *Let P be a tree-shaped polyomino consisting of N unit squares. We can decide in $O(N)$ time whether or not P is constructible.*

Proof. To keep track of the tiles that are and that become removable, we use a data structure that is initialized as follows:

Any free position that has an L_∞ -distance of at most two to any tile $t \in P$ gets the status ‘init’. Note that these are at most $O(N)$ many because each tile has at most 24 empty positions in distance at most two.

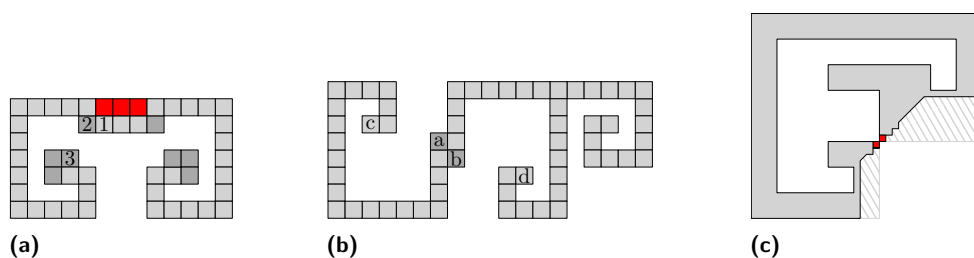
Starting from an empty position v that lies outside the bounding box of P , we perform a graph scan like BFS or DFS to get the set of all empty positions that are reachable from v and that are not adjacent to any tile from P . Let the status of these positions be ‘available’.

To identify tiles that are removable, we only have to check for each tile t the following: (i) t has only one neighbor in P , and (ii) t has an adjacent empty 1-blocked position, which is adjacent to a position with status ‘available’. This procedure costs $O(1)$ time per tile; thus $O(N)$ time in total.

Process the next steps iteratively, until no further tiles are removable. Let t be a removable tile.

1. Remove t from P and mark the position of t with ‘init’.
2. For each adjacent empty position p that is adjacent to an ‘available’ position but not to a tile of P :
 - a. Mark p as ‘available’ and start a graph scan on ‘init’ positions as well as mark them as ‘available’ if they are reachable from p but not adjacent to a tile of P .
 - b. During the scan, if an ‘init’ marked position does not change its state, check whether adjacent tiles become removable.

If these loops stop and there are still tiles left, we conclude that P is not constructible. Otherwise, P is constructible and the output is a feasible construction sequence.



■ **Figure 8** (a) No corner tile (dark gray) can be removed, because they either do not have a deconstruction step or are essential for connectivity. Successively removing the tiles 1, 2, and 3 by suitable deconstruction steps, the obtained shape can easily be deconstructed. Removing the red tiles first results in an indestructible shape. (b) By removing a first, we can remove the spiral starting with c and afterwards the rest. By removing b first, the spiral starting with d can be removed, but the remaining shape is indestructible. (c) For deconstruction, it is necessary to remove at least one of the red tiles. Independent from the scaling factor, both tiles block each other and we are only able to deconstruct a staircase to the right and below both tiles (hatched part).

Note that during a single graph scan each empty position can change its state only once, and the cost for each such position is constant. The constant cost of the checks in Step 2b can be charged to its adjacent ‘available’ position. Thus, over all iterations, each of the $O(N)$ positions is charged with cost $O(1)$ yielding a runtime of $O(N)$. ◀

It is easy to see that the same holds true for tree-shapes in 3D.

► **Corollary 16.** *Let P be a tree-shaped polycube consisting of N unit cubes. We can decide in $O(N)$ time whether or not P is constructible.*

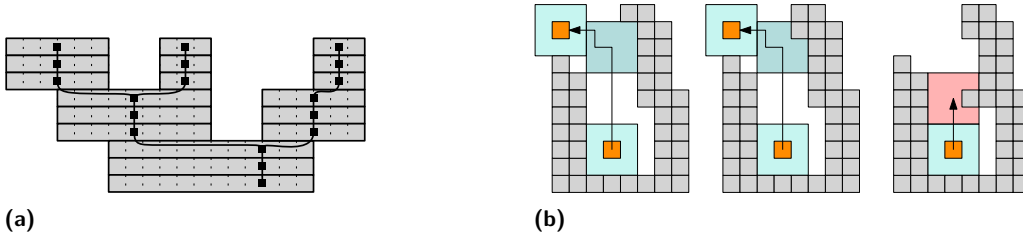
5.2 Scaled Shapes

Deciding constructibility of arbitrary polyominoes is more intricate than for tree-shaped polyominoes. On the one hand, it is not sufficient to restrict the search for removable tiles to *corner’s* (tiles with exactly one horizontal and one vertical neighbor), because for successfully deconstructing a polyomino, it may be necessary to remove non-corner tiles first, see Figure 8(a). On the other hand, removing non-corner tiles can result in an indestructible subshape, again see Figure 8(a). Furthermore, even in simple polyominoes, the removal of a corner tile can result in an indestructible polyomino, see Figure 8(b). Note that this is not the case if maximal movement is considered.

However, if scaling is allowed, we can show that the 2-scaled copy of a non-degenerate polyomino is constructible. Note that no scaling factor will suffice to guarantee constructibility for degenerate polyominoes, see Figure 8(c). Recall that in a non-degenerate polyomino P , for every pair $t_1, t_2 \in P$ of tiles that share exactly one point, $N[t_1] \cap N[t_2] \neq \emptyset$, i.e., t_1, t_2 have a common neighbor.

► **Definition 17.** *Let P be a polyomino and $c \in \mathbb{N}$. By P^c we denote the c -scaled copy of P , i.e., each tile in P is replaced by a $c \times c$ square of tiles.*

► **Definition 18.** *Let P be a polyomino. We call P c -empty if for any pair (p_1, p_2) of empty positions in the same connected component of $G_{\mathbb{Z} \setminus P}$, a square of size $c \times c$ can be moved from p_1 to p_2 without overlapping with P . We call P weakly c -empty if at any time at most one corner of the $c \times c$ square overlaps with a tile of P .*



■ **Figure 9** (a) The 3-scaled copy P^3 of a polyomino P (gray tiles), its partition into horizontal slabs \mathcal{S}_P , and its dual graph $\mathcal{C}(\mathcal{S}_P)$ (dark gray). (b) A polyomino that is 3-empty, weakly 3-empty, and not (weakly) 3-empty, respectively.

For an illustration of Definition 18, see Figure 9(b). For a 3-empty polyomino P , it is straightforward to see that as long as a tile $t \in P$ can be moved to an empty position p that lies in the outer face, such that all surrounding positions of p are empty as well, t can be removed from P . The intuition is the following: Consider a path of a 3×3 -square, centered at that empty position p , that connects p to the outside of the bounding box of P . The decomposition step for the tile t consists of all positions given by that path. Note that this still holds if we consider weakly 3-empty polyominoes.

We are able to show that we can always find such a removable tile, when P is the 2-scaled copy of a non-degenerate polyomino. One of the core ideas of our method is to make P weakly 3-empty. If P is weakly 3-empty, we consider a partition of P into horizontal slabs. Based on this partition, we can show that we can either remove a leaf of the dual graph of the partition, or we can *cut open* a hole of P , i.e., we remove two adjacent tiles to reduce the number of holes of P by 1.

► **Definition 19.** A slice of a polyomino P is the set of all tiles sharing the same x -coordinate. A slab is a maximal connected set of tiles within a slice.

► **Definition 20.** Let P be a polyomino, and \mathcal{S}_P the partition into slabs. By $\mathcal{C}(\mathcal{S}_P)$ we refer to the edge-contact graph of \mathcal{S}_P , i.e., each slab is represented as a vertex, and two vertices are connected if and only if the union of both slabs is connected.

It is straightforward to see that any leaf of $\mathcal{C}(\mathcal{S}_P)$ can be removed, if it lies in the outer face, and the polyomino is weakly 3-empty.

► **Lemma 21.** Let P be a non-degenerate polyomino that is weakly 3-empty. If $\mathcal{C}(\mathcal{S}_P)$ contains a degree-one vertex lying in the outer face, then the corresponding slab S can be removed from P .

Proof. Without loss of generality, we assume that there is no neighbor below S and that $P \setminus t$ is connected, where t is the rightmost tile of S . Arguments for the leftmost tile or if S has a neighbor below but no neighbor above are analogous.

Consider position p' of t and the position p which lies one step below and one step to the right of p' . Because S is weakly 3-empty, p is empty and also the center of a 3×3 square that contains t in the top-left corner. Also, because S has no neighbor on the bottom side and P is non-degenerate, we can move t to p by moving one step down and then one step right. From there, we can move t away from $P \setminus t$ by following the path of the 3×3 square. It is straightforward to see that $P \setminus t$ is still weakly 3-empty.

Because we can iteratively remove the leftmost or the rightmost tile of S without losing connectivity, we eventually remove S from P . ◀

► **Theorem 22.** *Let P be a non-degenerate polyomino. Then P^2 is constructible.*

Proof. The idea is the following. In a first phase we remove tiles from P^2 such that the remaining shape is 3-empty. In a second phase we deconstruct the remaining shape slab-wise. If the shape contains any holes, we cut them open.

We begin to describe **Phase 1**: Consider the set E_3 containing all empty positions that can build a pair with an empty position outside of the bounding box of P^2 to fulfill the weakly 3-empty property.

We will show how particles from P^2 can be removed such that any position in the outer face will belong to E_3 . As long as there are adjacent empty positions that are not in E_3 , repeat the following: Let $p_1, p_2 \notin E_3$ be two adjacent empty positions that both have a neighbor p'_1 , and p'_2 in E_3 . Without loss of generality, let (p_1, p_2) be a horizontal pair and let the neighbors are in the down direction. Then, to the left and to the right of (p'_1, p'_2) there are tiles $t_\ell, t_r \in P^2$ (or else $p_1, p_2 \in E_3$). Consider the maximal vertical line L of m tiles (t_1, \dots, t_m) ordered from bottom to top with $t_\ell \in L$ that have an empty position to the right. We make the following case distinction:

- (1.) $t_\ell = t_1$: We can remove t_ℓ by moving the tile one step to the right and down.
- (2.) $t_\ell \neq t_1$: We can remove the tile t below t_ℓ first by moving this tile two steps to the right. This position is the position below p'_2 , i.e., a position from E_3 . Furthermore, this position has to be the center of a 3×3 square containing only t_r . Thus, we can remove t from P^2 . After t is removed, we can move t_ℓ one step to the right, then down and right, reaching the same position.

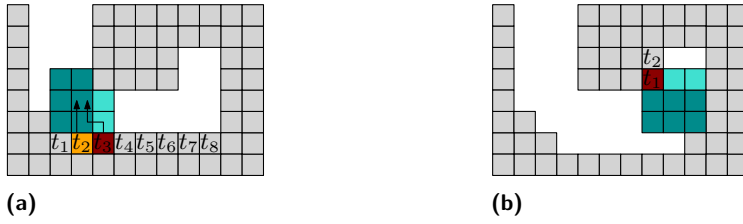
After removing t_ℓ , we can proceed by iteratively removing L completely. Note that in some cases t_1 or t_m may not be removable, because they lie in a corner. However, both empty positions to the right of them will be contained in E_3 , and thus, the narrow corridor is wide enough.

The cases when p_1, p_2 have their neighbors from E_3 in the direction up, or when they are a vertical pair, are handled analogously. We can always choose the line L in a way that L to the left, or to the down direction of (p'_1, p'_2) .

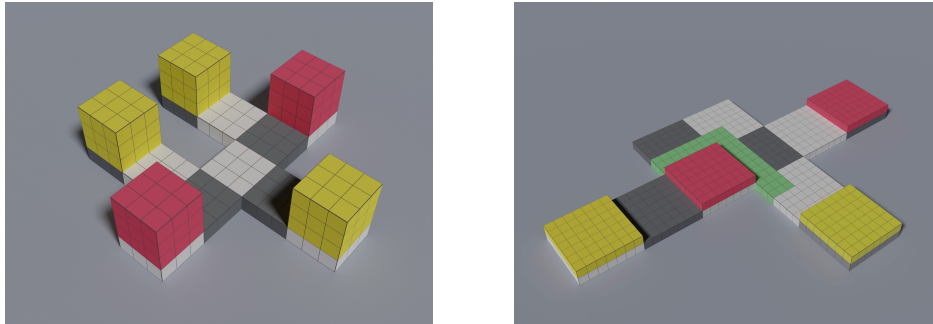
In **Phase 2**, we can assume that the remaining polyomino P' is weakly 3-empty. Thus, we can apply Lemma 21 to remove slabs of degree one. If there are no degree-one slabs, then we either removed every single tile, or there is a slab S incident to the outer face with k neighbors in $\mathcal{C}(\mathcal{S}_{P'})$ only on one side, whose removal would produce at most $k - 1$ connected components. This slab must exist. Otherwise, consider the set of all slabs S that have their neighbors in $\mathcal{C}(\mathcal{S}_{P'})$ on one side, and consider a maximal path in $\mathcal{C}(\mathcal{S}_{P'})$ between slabs from S . The slab S' on the end of this path has degree at least 2 in $\mathcal{C}(\mathcal{S}_{P'})$. Thus, we can extend the path until we reach another slab from S . By assumption, this slab cannot be a slab from the path, or else S' is a slab considered in (2). With this, we can always extend the path resulting in an infinite construction.

Now, consider a slab S as defined above. We know that there are two slabs S_1 and S_2 adjacent to S that belong to the same connected component in $P' \setminus S$. Without loss of generality, let S_1 be to the left of S_2 . We remove the first two tiles t_1 and t_2 from S that have a bigger x -coordinate than the rightmost tile in S_1 . There cannot be any tile above or below t_1 and t_2 because we consider a 2-scaled polyomino, and thus, this cannot break any connectivity. Also, any slab connected to S to the left of t_1 remains connected to any slab that is connected to S to the right of t_2 . This implies $P' \setminus \{t_1, t_2\}$ is a connected polyomino.

Unfortunately, $P' \setminus \{t_1, t_2\}$ is not weakly 3-empty anymore. By restarting Phase 1, we can continue to remove tiles. Because we are able to remove tiles in each case, we eventually deconstruct P^2 completely. Thus, P^2 is constructible. ◀



■ **Figure 10** (a) The vertical line $L = (t_1, \dots, t_8)$ with $t_\ell = t_3$. Cyan and teal positions must be empty, teal positions correspond to the pair (p'_1, p'_2) . The orange tile is removed first, followed the red tile. (b) Situation when $t_\ell = t_1$. We can immediately remove t_1 .



(a) Removing any white or gray 3×3 square disconnects a yellow part from the remaining polycube, resulting in a disconnected shape. (b) We cut out a 3×3 square from the white squares to avoid that the polycube becomes degenerate. Also note how yellow slabs are still connected through S_1 and S_2 .

■ **Figure 11** A slab S (lowest tiles) with slabs on top. Red slabs correspond to S_1 and S_2 of Phase 2 in the 2D algorithm. Yellow slabs are only connected by S .

Because there are (even tree-shaped) non-constructible polyominoes, this result is tight. If the polyomino is already 3-empty, we can skip the first phase. Whenever we have to cut open a hole, we remove three (instead of two) tiles, such that the property of being 3-empty is preserved. This results in the following corollary.

► **Corollary 23.** *Every non-degenerate, 3-empty polyomino is constructible.*

In 3D we cannot simply widen narrow corridors when scaled by a factor of 2. Therefore, we concentrate on adapting Phase 2 of the algorithm from Theorem 22 for shapes that are scaled by some constant factor to make corridors sufficiently wide. In contrast to 2D, a scaling factor of 3 may not be sufficient because the polycube can easily become disconnected when cycles in G_P (i.e., holes in 2D) are cut open (see Figure 11(a)). By using a higher scaling factor, i.e., at least seven, we can cut out a ditch of width 3 around S_1 (see green tiles in Figure 11(b)) leaving the remaining shape connected. More precisely, we cut through tiles that lie on a path between S_1 and S_2 through S . Note that a scaled tile, i.e., a 7×7 square, can be cut from two opposing sides while keeping the other two opposing sides connected (see Figure 11(b)). With this adaption we obtain the following.

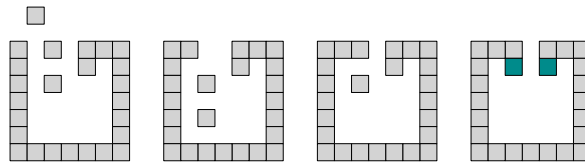
► **Theorem 24.** *Let P be a non-degenerate polycube. Then P^7 is constructible.*

6 Conclusion and Future Work

We provided a number of algorithmic results for assembling shapes by connecting particles to a seed tile. For future research several interesting problems remain open. What is the computational complexity of 2D-STAP? This is also an open question in the full tilt model [8]. Does 3D-STAP remain NP-hard when restricted to the class of non-degenerate shapes? We conjecture this to be true.

In this paper, we added one tile after the other to the seed. If this assumption is relaxed, i.e., more than one tile at a time can be added to the workspace, it is easy to see that more shapes are constructible, see Figure 12. Is there a classification of shapes that can be built in this model? This also leads to the question: "Which shapes are constructible by using pre-assembled shapes (e.g., trominoes, tetrominoes, etc.)?" By taking this a step further, we could also ask for a staged approach similar to [39], where whole subassemblies can attach to each other.

Another question arises by considering multiple seed tiles. What classes of shapes are constructible, if multiple seed tiles can be placed in advance, see Figure 12.



■ **Figure 12** The shape on the right is not constructible, if only one tile at a time is allowed to be controlled. If we can add multiple tiles simultaneously, the polyomino can be constructed from left to right by two down tilts followed by two up tilts. The polyomino is also constructible if we are allowed to place two (cyan colored) seed tiles in advance. Note that in this case even adding one tile at a time is sufficient to construct the polyomino.

References

- 1 P. K. Agarwal, B. Aronov, T. Geft, and D. Halperin. On Two-Handed Planar Assembly Partitioning. In *Proceedings of the Symposium on Discrete Algorithms*, 2021.
- 2 J. Balanza-Martinez, T. Gomez, D. Caballero, A. Luchsinger, A. A. Cantu, R. Reyes, M. Flores, R. Schweller, and T. Wylie. Hierarchical Shape Construction and Complexity for Slidable Polyominoes under Uniform External Forces. In *Proceedings of the Symposium on Discrete Algorithms*, 2020.
- 3 J. Balanza-Martinez, A. Luchsinger, D. Caballero, R. Reyes, A. A. Cantu, R. Schweller, L. A. Garcia, and T. Wylie. Full Tilt: Universal Constructors for General Shapes with Uniform External Forces. In *Proceedings of the Symposium on Discrete Algorithms*, 2019.
- 4 A. T. Becker, E. D. Demaine, S. P. Fekete, G. Habibi, and J. McLurkin. Reconfiguring Massive Particle Swarms with Limited, Global Control. In *International Symposium on Algorithms and Experiments for Sensor Systems, Wireless Networks and Distributed Robotics*, 2013.
- 5 A. T. Becker, E. D. Demaine, S. P. Fekete, J. Lonsford, and R. Morris-Wright. Particle computation: complexity, algorithms, and logic. *Natural Computing*, 2019.
- 6 A. T. Becker, E. D. Demaine, S. P. Fekete, and J. McLurkin. Particle computation: Designing worlds to control robot swarms with only global signals. In *International Conference on Robotics and Automation*, 2014.
- 7 A. T. Becker, S. P. Fekete, L. Huang, P. Keldenich, L. Kleist, D. Krupke, C. Rieck, and A. Schmidt. Targeted Drug Delivery: Algorithmic Methods for Collecting a Swarm of Particles

- with Uniform, External Forces. In *International Conference on Robotics and Automation*, 2020.
- 8 A. T. Becker, S. P. Fekete, P. Keldenich, D. Krupke, C. Rieck, C. Scheffer, and A. Schmidt. Tilt Assembly: Algorithms for Micro-Factories that Build Objects with Uniform External Forces. *Algorithmica*, 2018.
 - 9 A. T. Becker, O. Felfoul, and P. E. Dupont. Simultaneously powering and controlling many actuators with a clinical mri scanner. In *International Conference on Intelligent Robots and Systems*, 2014.
 - 10 A. T. Becker, O. Felfoul, and P. E. Dupont. Toward tissue penetration by mri-powered millirobots using a self-assembled gauss gun. In *International Conference on Robotics and Automation*, 2015.
 - 11 A. T. Becker, Y. Ou, P. Kim, M. J. Kim, and A. Julius. Feedback control of many magnetized: *Tetrahymena pyriformis* cells by exploiting phase inhomogeneity. In *International Conference on Intelligent Robots and Systems*, 2013.
 - 12 I. D. Brown, J. G. Connolly, and G. Kerkut. Galvanotaxic response of *tetrahymena vorax*. *Comparative Biochemistry and Physiology Part C: Comparative Pharmacology*, 1981.
 - 13 D. Caballero, A. A. Cantu, T. Gomez, A. Luchsinger, R. Schweller, and T. Wylie. Building Patterned Shapes in Robot Swarms with Uniform Control Signals. In *Proceedings of the Canadian Conference on Computational Geometry*, 2020.
 - 14 D. Caballero, A. A. Cantu, T. Gomez, A. Luchsinger, R. Schweller, and T. Wylie. Hardness of reconfiguring robot swarms with uniform external control in limited directions. *Journal of Information Processing*, 2020.
 - 15 D. Caballero, A. A. Cantu, T. Gomez, A. Luchsinger, R. Schweller, and T. Wylie. Relocating Units in Robot Swarms with Uniform Control Signals is PSPACE-complete. In *Proceedings of the Canadian Conference on Computational Geometry*, 2020.
 - 16 S. Cannon, E. D. Demaine, M. L. Demaine, S. Eisenstat, M. J. Patitz, R. T. Schweller, S. M. Summers, and A. Winslow. Two Hands Are Better Than One (up to constant factors): Self-Assembly In The 2HAM vs. aTAM. In *Proceedings of the International Symposium on Theoretical Aspects of Computer Science*, 2013.
 - 17 C. Chalk, E. Martinez, R. Schweller, L. Vega, A. Winslow, and T. Wylie. Optimal staged self-assembly of general shapes. *Algorithmica*, 2018.
 - 18 C. Chalk, E. Martinez, R. Schweller, L. Vega, A. Winslow, and T. Wylie. Optimal staged self-assembly of linear assemblies. *Natural Computing*, 2019.
 - 19 A. Chanu, O. Felfoul, G. Beaudoin, and S. Martel. Adapting the clinical mri software environment for real-time navigation of an endovascular untethered ferromagnetic bead for future endovascular interventions. *Magnetic Resonance in Medicine: An Official Journal of the International Society for Magnetic Resonance in Medicine*, 2008.
 - 20 U. K. Cheang, D. Roy, J. H. Lee, and M. J. Kim. Fabrication and magnetic control of bacteria-inspired robotic microswimmers. *Applied Physics Letters*, 2010.
 - 21 H.-L. Chen and D. Doty. Parallelism and time in hierarchical self-assembly. In *Proceedings of the Symposium on Discrete Algorithms*, 2012.
 - 22 M. de Berg and A. Khosravi. Optimal binary space partitions for segments in the plane. *International Journal on Computational Geometry and Applications*, 2012.
 - 23 E. D. Demaine, M. L. Demaine, S. P. Fekete, M. Ishaque, E. Rafalin, R. T. Schweller, and D. L. Souvaine. Staged self-assembly: nanomanufacture of arbitrary shapes with $O(1)$ glues. *Natural Computing*, 2008.
 - 24 E. D. Demaine, S. P. Fekete, C. Scheffer, and A. Schmidt. New geometric algorithms for fully connected staged self-assembly. *Theoretical Computer Science*, 2017.
 - 25 D. Doty. Theory of algorithmic self-assembly. *Communication of the ACM*, 2012.
 - 26 R. Dreyfus, J. Baudry, M. L. Roper, M. Fermigier, H. A. Stone, and J. Bibette. Microscopic artificial swimmers. *Nature*, 2005.

- 27 A. Ghosh and P. Fischer. Controlled propulsion of artificial magnetic nanostructured propellers. *Nano letters*, 2009.
- 28 P. Keldenich, S. Manzoor, L. Huang, D. Krupke, A. Schmidt, S. P. Fekete, and A. T. Becker. On designing 2d discrete workspaces to sort or classify polyominoes. In *International Conference on Intelligent Robots and Systems*, 2018.
- 29 P. S. S. Kim, A. T. Becker, Y. Ou, A. A. Julius, and M. J. Kim. Swarm control of cell-based microrobots using a single global magnetic field. In *International Conference on Ubiquitous Robots and Ambient Intelligence*, 2013.
- 30 P. S. S. Kim, A. T. Becker, Y. Ou, A. A. Julius, and M. J. Kim. Imparting magnetic dipole heterogeneity to internalized iron oxide nanoparticles for microorganism swarm control. *Journal of Nanoparticle Research*, 2015.
- 31 A. V. Mahadev, D. Krupke, J.-M. Reinhardt, S. P. Fekete, and A. T. Becker. Collecting a Swarm in a Grid Environment Using Shared, Global Inputs. In *International Conference on Automation Science and Engineering*, 2016.
- 32 S. Manzoor, S. Sheckman, J. Lonsford, H. Kim, M. J. Kim, and A. T. Becker. Parallel Self-Assembly of Polyominoes Under Uniform Control Inputs. *Robotics and Automation Letters*, 2017.
- 33 S. Martel, O. Felfoul, J.-B. Mathieu, A. Chanu, S. Tamaz, M. Mohammadi, M. Mankiewicz, and N. Tabatabaei. Mri-based medical nanorobotic platform for the control of magnetic nanoparticles and flagellated bacteria for target interventions in human capillaries. *The International journal of robotics research*, 2009.
- 34 M. J. Patitz. An introduction to tile-based self-assembly and a survey of recent results. *Natural Computing*, 2014.
- 35 K. E. Peyer, S. Tottori, F. Qiu, L. Zhang, and B. J. Nelson. Magnetic helical micromachines. *Chemistry—A European Journal*, 2013.
- 36 K. E. Peyer, L. Zhang, and B. J. Nelson. Bio-inspired magnetic swimming microrobots for biomedical applications. *Nanoscale*, 2013.
- 37 P. W. Rothmund. Design of DNA origami. In *International Conference on Computer-Aided Design*, 2005.
- 38 P. W. Rothmund and E. Winfree. The program-size complexity of self-assembled squares. In *Proceedings of the Symposium on Theory of Computing*, 2000.
- 39 A. Schmidt, S. Manzoor, L. Huang, A. T. Becker, and S. P. Fekete. Efficient Parallel Self-Assembly Under Uniform Control Inputs. *Robotics and Automation Letters*, 2018.
- 40 R. Schweller, A. Winslow, and T. Wylie. Nearly constant tile complexity for any shape in two-handed tile assembly. *Algorithmica*, 2019.
- 41 H. M. Shad, R. Morris-Wright, E. D. Demaine, S. P. Fekete, and A. T. Becker. Particle computation: Device fan-out and binary memory. In *International Conference on Robotics and Automation*, 2015.
- 42 E. Steager, C.-B. Kim, J. Patel, S. Bith, C. Naik, L. Reber, and M. J. Kim. Control of microfabricated structures powered by flagellated bacteria using phototaxis. *Applied Physics Letters*, 2007.
- 43 P. Vartholomeos, M. R. Akhavan-Sharif, and P. E. Dupont. Motion planning for multiple millimeter-scale magnetic capsules in a fluid environment. In *International Conference on Robotics and Automation*, 2012.
- 44 P. Vartholomeos, C. Bergeles, L. Qin, and P. E. Dupont. An mri-powered and controlled actuator technology for tetherless robotic interventions. *The International Journal of Robotics Research*, 2013.
- 45 H. Wang. Proving theorems by pattern recognition—II. *Bell System Technical Journal*, 1961.
- 46 D. B. Weibel, P. Garstecki, D. Ryan, W. R. DiLuzio, M. Mayer, J. E. Seto, and G. M. Whitesides. Microoxen: Microorganisms to move microscale loads. *Proceedings of the National Academy of Sciences*, 2005.
- 47 E. Winfree. *Algorithmic self-assembly of DNA*. PhD thesis, CalTech, 1998.

- 48 D. Woods. Intrinsic universality and the computational power of self-assembly. *Philosophical Transactions of the Royal Society A: Mathematical, Physical and Engineering Sciences*, 2015.
- 49 L. Zhang, J. J. Abbott, L. Dong, B. E. Kratochvil, D. Bell, and B. J. Nelson. Artificial bacterial flagella: Fabrication and magnetic control. *Applied Physics Letters*, 2009.
- 50 L. Zhang, K. E. Peyer, and B. J. Nelson. Artificial bacterial flagella for micromanipulation. *Lab on a Chip*, 2010.